https://doi.org/10.33261/jaaru.2019.26.1.020 *Association of Arab Universities Journal of Engineering Sciences (2019) 26(1): 150–159*

Association of Arab Universities Journal of Engineering Sciences

مجلة اتحاد الجامعات العربية للدراسات والبحوث الهندسية

Effect of Shoulder–Workpiece Interference Depth on the Quality of Friction Stir Welding of AA7075-T6 Aluminium Alloy

Abbas Akram Abbas [1,*], **and** ***Hazim H. Abdulkadhum*** [2]

[1] *Department of Mechanical Engineering, University of Baghdad, Baghdad, Iraq, abbas.akram.aa@gmail.com*

[2] *General Directorate of Vocational Education, Ministry of Education, Baghdad, Iraq, hhabdulkadhum@gmail.com*

** Corresponding author: Abbas Akram Abbas, abbas.akram.aa@gmail.com*

Published online: 31 March 2019

Abstract— The joining of high strength aluminium alloy AA7075-T6 sheets of 3 mm thickness was an attempt utilizing friction stir welding process. The effect of interference depth between tool shoulder and surface workpiece on the welding quality and its effect on the mechanical and metallography properties of welded joints were studied. This process is carried out using a composite tool consists of a concave shoulder made of H13 tool steel and cylindrical left-hand thread with 1mm pitch pin (probe) made of cobalt-based alloy MP159. The dimensions of tools were 14mm shoulder diameter and the pin has 5mm diameter and 2.7mm length. The tool rotation speed and welding speed were 981 rpm 169 mm/min respectively, and the tilt angle was 2°. The range of interference depth between the shoulder and workpiece was selected (0.05, 0.1, 0.15, 0.2, 0.25, and 0.3) mm. various tests were executed to evaluate the welding quality. The results show that lack of filling defect appeared on the welding surface at the interference depth 0.05 mm. An invisible tunnel and lack of penetration in the bottom of the stir zone appeared when the interference depths were 0.1 mm and 0.15 mm. Defect-free welds obtained when interference depths were (0.2, 0.25, and 0.3) mm. The welding efficiency of the defect-free welds was in the range (85.3-92.3%) depending on the ultimate tensile strength of the parent alloy.

Keywords— AA7075, Friction stir welding, Shoulder–Workpiece interference depth, Plunge depth, Fixture.

1. Introduction

Friction stir welding (FSW) was invented at the welding institute (TWI) of the United Kingdom in 1991 as a solid-state joining technique [10], that fabricate a weld between two (or more) workpieces (WPs) due to heating and plastic material displacement produced by a rapidly rotating tool that traverses the weld joint. Even though the friction stir welding technique was initially applied to aluminium alloys, and it is developed to join other metals, including magnesium, copper, zinc, bronze, titanium, lead, and steels, as well as polymers and composites [5] [8].

The FSW can weld either butt or lap joints in a broad range of materials thickness and lengths [14]. It is used to weld dissimilar materials combinations, specifically those with close melting temperatures and comparable behavior such as hot workability [1]. Many alloys cannot be welded by fusion welding but can be welded through friction stir welding process [16]. Novel trials have demonstrated that FSW can be utilized to join aluminium and its alloys up to 75mm plate thickness in a single pass, opening up the innovation to new applications [6]. Development of friction stir welding throughout the years to weld a very large range of structures/parts and a wide range of weld geometry, has been sophisticated rapidly, and having a good grip on some prestigious research centers in the world [9].

In principle, FSW is a very simple process. Two pieces of sheet or plate material are butted together (lap and other configurations are also used) and clamped to a rigid backing plate onto the work table of FSW machine to prevent the abutting or other configuration joint faces from being forced apart or in any other way moved out of position. The FSW process includes four major stages: plunge stage, dwell stage, welding stage and cooling stage (pull out the tool) [15] [3].

A non-weldable heat-treated AA7075-T6 aluminium alloy has high strength compared to some types of steel, average machinability, good fatigue strength, and lower corrosion resistance compared with other aluminium alloys but better corrosion resistance than the 2000 series. AA7075-T6 has high-strength and low-density, so it is widely used in an aerospace and transportation manufacturing to form top surface of aircraft, most of original frames and

structures attached to the landing gear to the fuselage, automobile framework structures, seatbelt hinges, links, bobbins, retractors, and mold tool manufacturing[11] [7] [13].

A range of parameters are affected on the welding process including tool rotation speed (TRS), welding speed (WS), shoulder plunge depth; these parameters have a significant effect on heat generation [4]. To obtain the good welding quality the TRS and WS were mostly optimized to control on the heat input as much as possible and prevent formation the defects during FSW process. Imputed that the value of shoulder-WP interference depth is largely determined the quality of welding surface. If the shoulder-WP interference is too high or too low, weld surface defects such as groove, flash and internal defects such as tunnel or void are more prone to be formed in the weld line. Actually, the worth of shoulder-WP interference reflects the scope of interaction between tool shoulder and WP thereby on the heat generation that effects on welding quality [17].

Derazkola et al. [2] investigated the influence of shoulder plunge depth (SPD) on the mechanical properties of FSW of A441 AISI steel with AA1100 aluminium alloy. For a selected range of shoulder plunge depth 0.1, 0.2, 0.4, and 0.6 mm and other welding process parameters are constant. The results show that when the SPD increases, the heat generation increased and the grain size in SZ is decreased. Depending on the tensile test it is shown that the highest tensile strength value is at SPD 0.22 mm. Ramulu et al. [12] studied the effect of shoulder diameter and plunge depth on the formability of friction-stir-welded sheets for AA6061-T6. The results showed that the increase in shoulder diameter and plunge depth, the forming limit improved frequently.

Zevanathan and Babu [18] proved that when weld AA 6063 aluminium alloy by FSW process, the increase in SPD lead to decrease in the mechanical properties, and excessive flash is formed on the outer surface of the weld.

The aim of this work is to study the effect of shoulder-workpiece interference (SWI) depth on the mechanical properties and observe the defects free joint during a microstructure of the weldments.

2. Experimental Work

In this work, the AA7075–T6 aluminium alloy rolled sheets of 3 mm thickness were used as a base material for the butt joint welding process. A chemical composition of the welded sheets was listed in the **Table 1** and the mechanical properties are mentioned in the **Table 2**. The specimens to be welded were cut and machined to the final dimensions (200×100×3) mm, considering the rolling direction is perpendicular to the welding direction.

The composite tool consists of two separate parts shoulder and pin (probe). A concave surface shoulder 6º, made of ASTM H13 chromium–molybdenum hot worked air hardening steel with 15mm diameter, the pin material is Cobalt-based superalloy MP159, left-hand threaded, cylindrical flat end, 1mm threaded pitch, 5mm diameter, and 2.7mm length. The FSW was executed on a CNC vertical milling machine type MITSUBISHI M70V. For the reason of a fixed spindle head, a special designed and manufactured adjustable-angle fixture was designed and manufactured included a backing plate. It can be tilted by a range of inclinations included but not limited to 2º. The WP is fixed rigidly in the space between the back plate and the upper part of the fixture by means of upper and side sets of screws as shown in Figure 1.

Table 1: Chemical compositions of AA7075-T6.

Element%	Si	Fe	Cu	Mn	Mg	Cr	Zn	Ti	Other	Al
Measured	0.101	0.332	1.73	0.075	2.44	0.213	5.68	0.031	0.056	Bal.
Standard	≤ 0.4	≤ 0.5	1.2-2.0	≤ 0.30	2.1-2.9	0.18-0.28	5.1-6.1	0.2	0.056	Bal.

Table 2: Mechanical properties of AA7075-T6.

	Tensile Yield Strength (MPa)	Ultimate Tensile Strength (MPa)	Vickers Hardness (HV)
Actual value	496	525	170
Standard	470 min	510 min	165 min

The range of shoulder-WP interference (SWI) depths of (0.05, 0.1, 0.15, 0.2, 0.25, and 0.3) mm was applied in this work and other parameters remain constant in all process as listed in the **Table 3**.

3. Non-Destructive Tests

3.1 Visual test

Visual examination of the face and root of the weld was carried out. Specimens containing visible defects are excluded from the other tests.

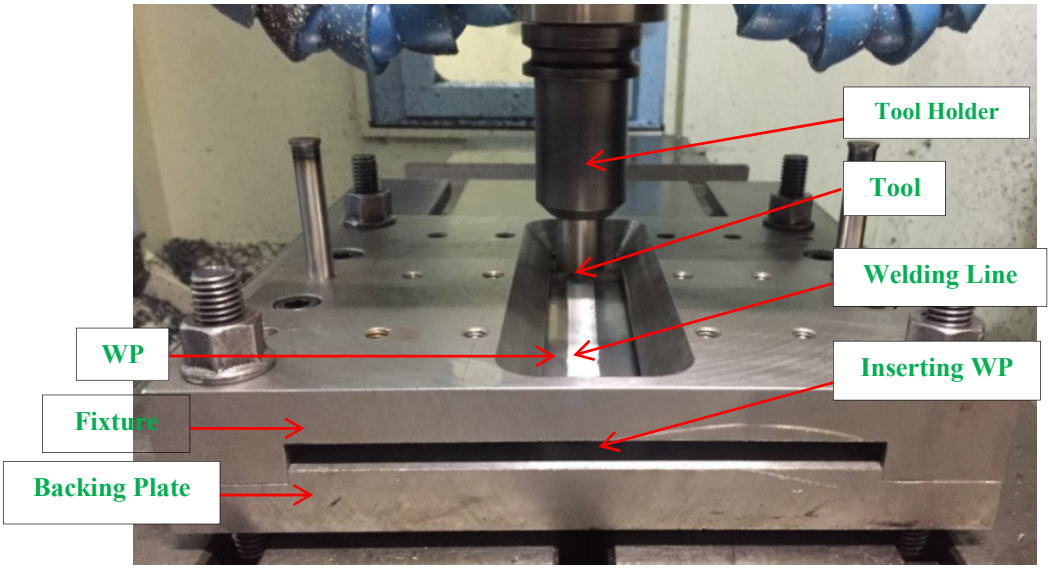

Figure 1: Set up the backing plate, fixture, and WP in the CNC milling machine

Table 3: The parameters used in FSW process.

Joint configuration	Butt joint
Material welded	AA7075-T6
WP length (mm)	200
WP width (mm)	100
WP thickness (mm)	3
Length of welds (mm)	165
TRS (rpm)	981
WS (mm/min)	159
Tool rotation direction	CW
Tilt angle (deg)	2
Shoulder diameter (mm)	14
Shoulder concave angle (deg)	6
Pin configuration	Cylindrical, threaded and flat end
Pin diameter (mm)	5
Pin length (mm)	2.7
Pin thread type	Left hand
Welding direction	Perpendicular to the rolling direction
Tool offset (mm)	0

3.2 Radiographic Test

X-ray is employed in the radiographic test to penetrate an object and detect any discontinuities by the resulting image on a viewing or recording. A fluorescent screen is a viewing medium, the source energy depends on its thickness, and density of used metal, the energy supplied in this test of 3 mm thick welded sheets was 150 kV and 2.2 mA according to ASTM 1A/SWSI. X-ray radiography test is used to reveal many internal defects such as tunnels, voids, cracks, and others.

4. Macrostructure and Microstructure Evaluation

A macrostructure and microstructure tests were performed on the specimens that prepared from the cross-section perpendicular to the welding direction to the required sizes and mounted on Bakelite for easy preparing. Grinding process was carried out by using emery papers of silicon carbide (SiC) of various grits namely (400, 500, 600, 800, 1000, 1200, and 1500). Then a polishing was carried out using the diamond mash of particle size of 0.5 µm. Followed by etching stage included immersion of specimen into etching solution by using Keller's reagent (2ml HF, 3ml HCl, 5ml HNO3, and 190ml water).

5. Destructive Tests

5.1 Tensile test

Flat tensile test specimens were cut perpendicular to the weld line using CNC wire EDM machine. The specimens are prepared for final dimensions according to ASTM (E8/E8M – 09) as shown in the **Figure** 2. All tensile tests were executed at room temperature and constant loading rate of 1 mm/min. The tests executed on the universal testing machine type (LARYEE) of maximum capacity 50kN.

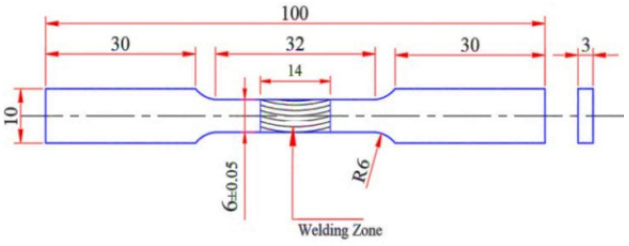

Figure 2: Standard Tensile specimen according to ASTM (E8/E8M-09)

5.2 Bending Test

The three-point bending test for surface and root of welds using the universal testing machine were carried out. The specimen dimensions were (150x100x3) mm.

The bending tests were done as per ASTM E-290-97a for the welded specimens to check ductility of welding zones and to detect the existence of subsurface defects because of these tests are very sensitive to defects near the weld surface, such as root defect.

5.3 Micro-hardness test

The digital micro-hardness tester was used to measure Vickers hardness (HV) with 1.96N load at 15 seconds. The test was performed on a centerline of a cross-section perpendicular to the welding direction, this test included the regions nugget zone (NZ), thermal mechanical affected zone (TMAZ), heat affected zone (HAZ), and base metal (BM). Micro-hardness profile is registered at intervals of 1mm between the neighboring measurements.

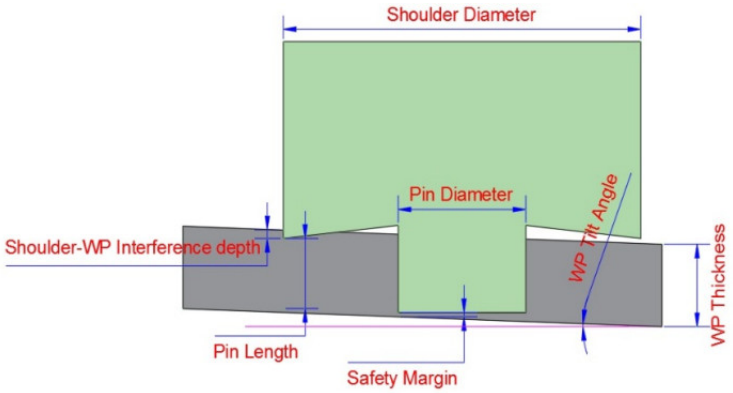

Figure 3: Significant definitions that affect the FSW process

Table 4: listed the different shoulder-WP interference depths.

Specimen no.	Pin Length (mm)	Shoulder-WP Interference depth (mm)	Safety Margin (mm)	Tilt angle
13	2.7	0.05	0.4	2°
14	2.7	0.10	0.35	2°
15	2.7	0.15	0.3	2°
16	2.7	0.20	0.25	2°
17	2.7	0.25	0.2	2°
18	2.7	0.30	0.15	2°

6. Results and Discussions

This work included the change in the SWI depth as shown in **Fig. 3** and listed in the **Table. 4**.

6.1 Visual test results

After accomplished the welding process, visual inspection was attempted for all six cases after the welding process is accomplished. The results showed that in the specimen no. 13 when SWI depth was (0.05) mm, it is found that there is lack of filling defect in the weld surface as shown in Figure 4, because of the contact area between tool shoulder and WP was very low which led to decrease in friction heat and plunge force. The other specimens were accepted in the visual inspection as shown in Figure 5.

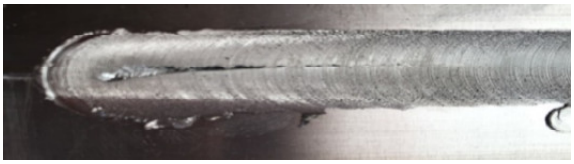

Figure 4: Specimen no.13 lack of filling defect.

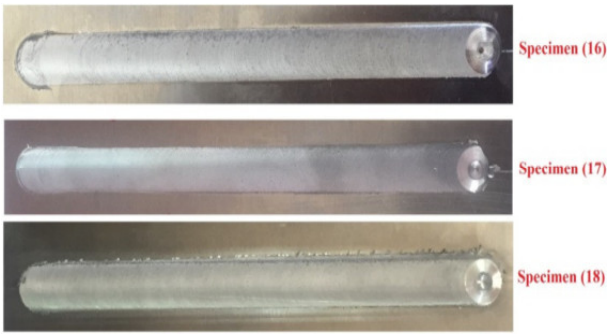

Figure 5: Defect-Free specimens nos. 16, 17, and 18.

6.2 X-Ray Radiographic test results

In this test, the accepted welds of the visual test were tested by X-Ray; the test was executed to specimens nos.14, 15, 16, 17, and 18. The results show that in the specimen no. 14 at SWI depth of 0.1 mm an internal tunnel defect is presented as shown in Figure 6A because of insufficient heat generation and low plunge force. Other specimens nos. 15, 16, 17, and 18 were accepted in this test, Figure 6 B show that accepted specimen is no. 15.

6.3 Macrostructure and Microstructure Test Results

Accepted specimens (nos. 15,16,17, and 18) were tested in X-Ray test using an optical microscope to check carefully the defects that did not appear in the previous tests. In specimen no.16 when SWI depth is 0.15 mm, lack of penetration at the weld root as shown in Figure 7 because of insufficient plunge pin tool in the weld zone. This led to inadequate material deformation to consume the bond line. It is noted the absence of defects in the welding zone the specimens nos. 16, 17, and 18 as shown in Figure 8 because of SWI depths were sufficient and the plunging forces were sufficient for the required heat generation, forging force, and the metal flow between the faying surfaces.

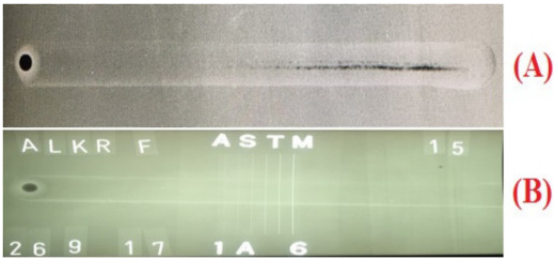

Figure 6: X-Ray for specimens nos. 14 and 15

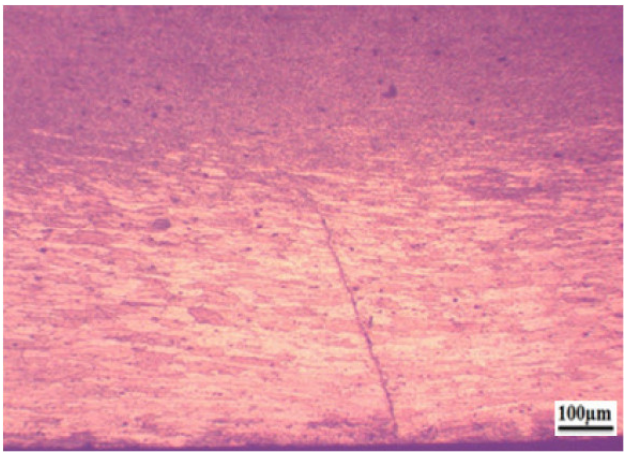

Figure 7: Microstructure image shows Lack of penetration defect (Magnification X = 140).

An oval-shaped area at the center of the weld is appeared as shown in **Figure 8a** where the pin of the FSW tool passed through, and mixed the material together. Moreover fully re-crystallized at the weld center is reforted. Equiaxed grain in smaller size shown in the microstructure of (NZ) comparing with the base material, **Figure 8b** and in the TMAZ the grain has been no dynamic recrystallization, and instead, the grains are elongated and typically of a different orientation than those in the base metal as shown in **Figure 8c**, d, in additional to note the region no significant change in grain size or orientation when compared with BM called heat affected zone (HAZ) as shown in **Figure 8c**, d. The microstructure image of BM is presented in **Figure 9**.

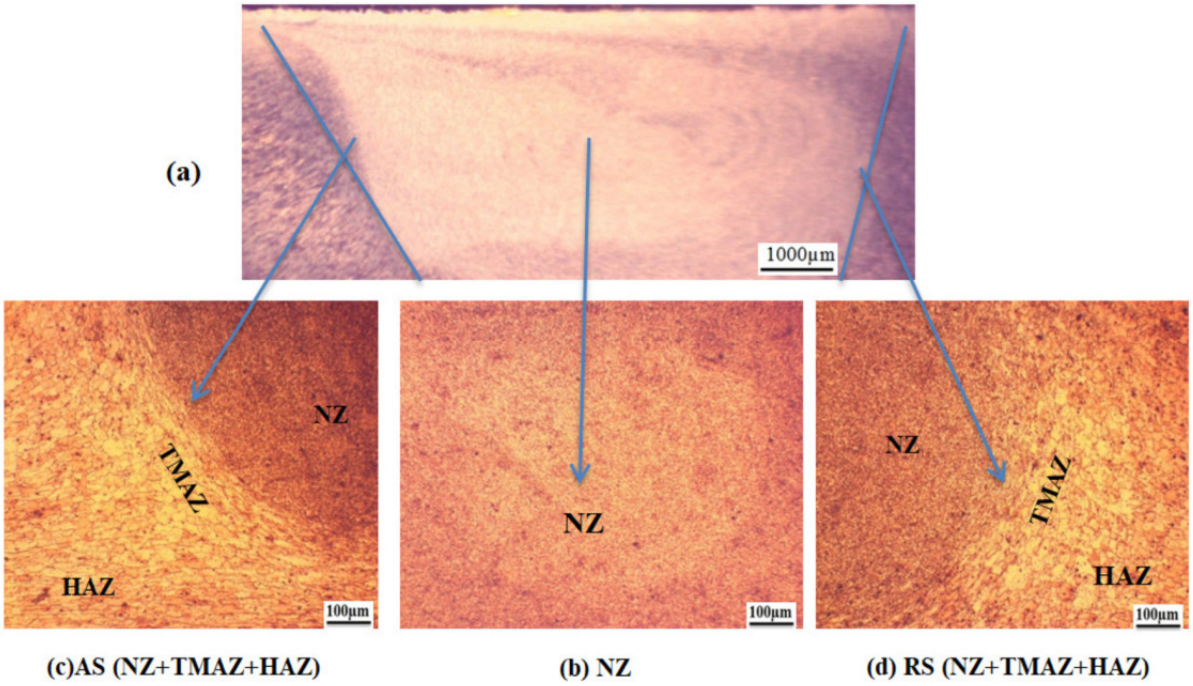

Figure 8: Microstructure of the base metals AA7075-T6 (Magnification X = 140).

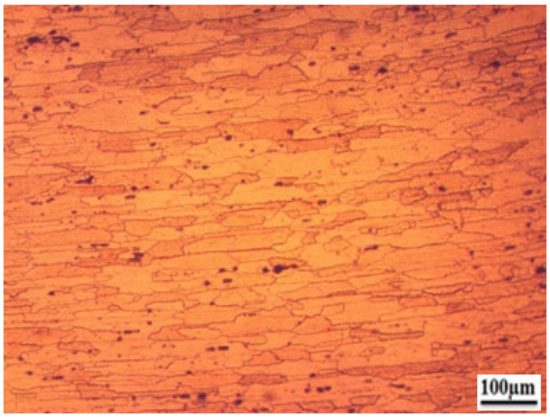

Figure 9: Microstructure of weld zones (Magnification X = 140).

6.4 Tensile Test Results

The results of the transverse tensile test are summarized in **Table 5**. In general, both yield strength and ultimate tensile strength were reduced in the welded area compared with that for parent material, due to a combination of dissolution, coarsening and precipitate of strengthening precipitates during FSW or localized deformation, considering that the welded aluminium alloys AA7075-T6 is age hardened alloys. This means a drop in the mechanical property is expected due to the heat generated during the FSW process. The tensile test performed on the defect-free weld in specimens nos. (16, 17, and 18) indicates highest tensile stress at SWI depth 0.25 mm because of sufficient plunge force and heat generation with good stirring and refine the grain in the welding zone while, decrease when SWI depth increase to 0.30 mm, because of thinning in nugget zone. The highest welding efficiency was 92.337% in specimen no. 17 when SWI depth 0.25mm based on ultimate tensile stress. The specimens were fractured from the retreating side of the HAZ zone as shown in **Figure 10** during tensile tests. No plastic deformation in HAZ but has only been subjected to the thermal cycle. Due to overaged and coarsen strengthening precipitates and localized deformation leading to degradation of mechanical properties (reduced strength and ductility) in the HAZ. The behavior of welded metal during the tensile test as shown in **Figure 11**, and the effect of SWI depth on the welding efficiency as shown in **Figure 12**. The efficiency of welding was calculate by using the equ. (1).

Welding Efficiency = ((UTS) for weld joint)/((UTS) for parent metal)×100% (1)

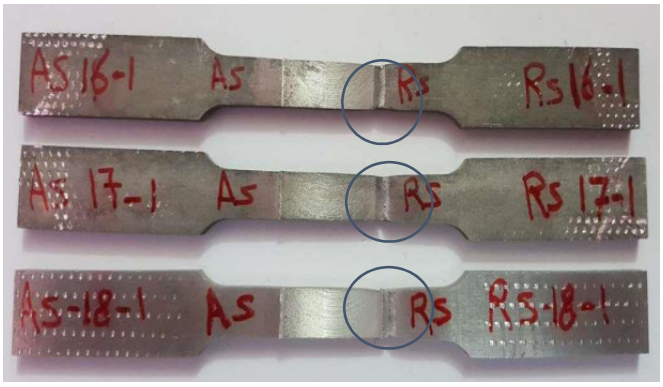

Figure 10: Tensile specimens nos. (16, 17, and 18) after fracture

Table 5: Results of tensile test for the parent metals and FSW tests.

Specimen no.	SWI depth (mm)	Yield Stress (MPa)	UTS (MPa)	Elong. at Fracture %	Defects	Welding Efficiency (%)
BM	-	496	525	7.23	-	100
16	0.2	341	447.8	3.50	Defect -free	85.30
17	0.25	361	484.8	5.52	Defect -free	92.34
18	0.3	341	470.7	5.13	Defect -free	89.65

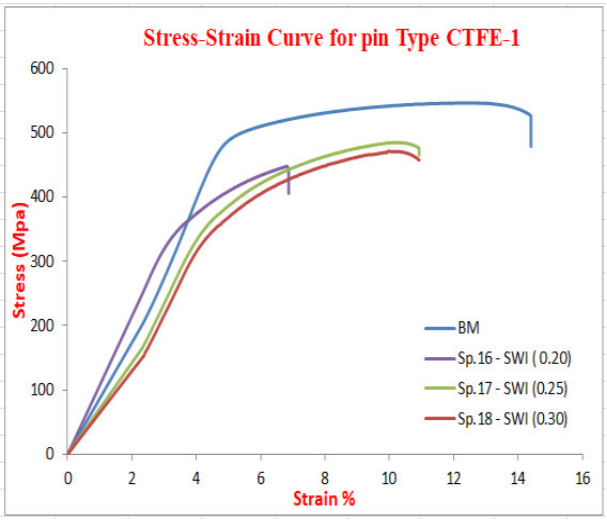

Figure 11: Stress-Strain curve for BM and specimens nos. (16, 17, and 18).

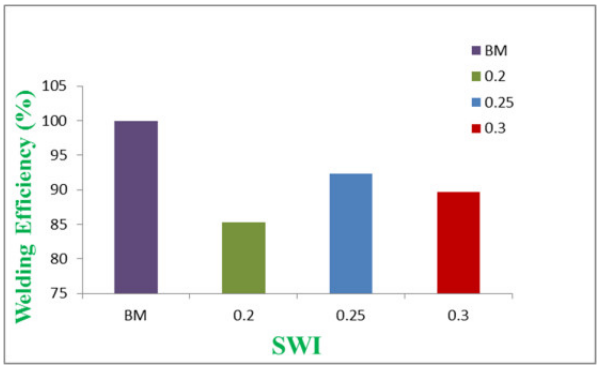

Figure 12: Welding efficiency depended on the tensile stress

6.5 Bending Test Results

Defect-free welds were subjected to the three-point bending test using the universal testing machine (LARYEE). The bending tests are done as per ASTM E-290-97a for the welded specimens to check ductility of welding zones and to detect the existence of subsurface defects because of these tests are very sensitive to defects near the weld surface, such as root defect. The result shows that no defects were detected in all joints in booth surface and root bending test. The best mechanical properties are reforted for specimen no. 17 at WSI depth 0.25 mm for face bending while they are decreased when increasing SWI depth to 0.3 mm. The results are collected in **Table 6** and the behavior of metal during face bending, root bending and welding efficiency for bending test are shown in **Figure 13**, **Figure 14**, and **Figure 15** respectively. Also it is noted that the slight difference between the result of the face and root bending. Also, the bending angle of BM was 111° and the specimens nos. 16, 17, and 18 were 107°, 107°, and 106° respectively, that means the ductility of BM is more than the weld because of spring back occurs in BM. **Figure 16** shows the specimens after bending test.

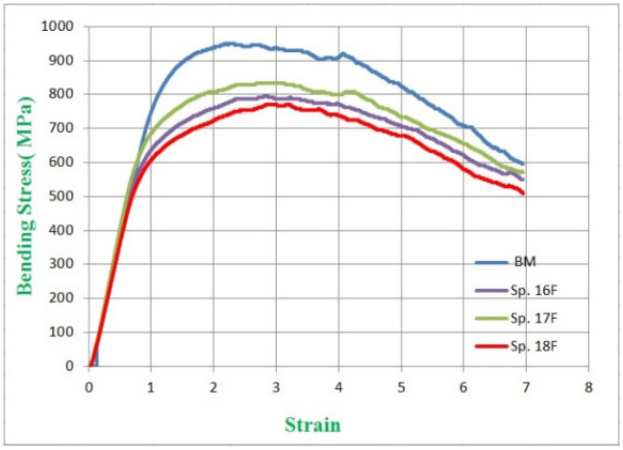

Figure 13: Stress-strain curve for face bending

Table 6: Result of Bending Tests.

Specimen no.	SWI depth (mm)	Ultimate Bending stress (Face) (MPa)	Ultimate Bending stress (Root) (MPa)	Bending Angle (degree)	Welding Efficiency Face %	Welding Efficiency Root %
BM		950	950	111°	100	100
16	0.2	795.8	795.8	107°	83.8	83.8
17	0.25	835	800	107°	87.9	84.2
18	0.3	770.8	758	106°	81.1	79.8

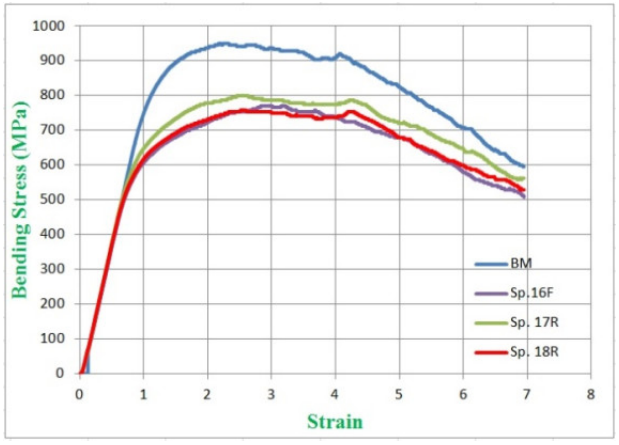

Figure 14: Stress-strain curve for root bending

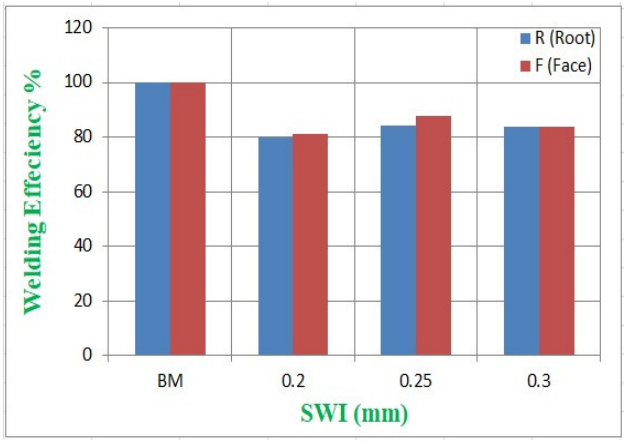

Figure 15: Welding efficiency for bending test.

6.6 Micro-Hardness Test Results

The FSW is a process accompanied by generating elevated temperature which leads to grain refinement and other thermal changes in the weld zone, therefore, the hardness results were changed through the weld zone as shown in **Figure 17**. In general, due to heat generated during the FSW, the hardness of all welded specimens in the NZ is less than those of base material. The NZ hardness is higher than the TMAZ and HAZ because of fine grain size in the NZ as per the Hall-Petch equation, when the grain size decreases, the hardness increases and some of the second phase is precipitated while in the TMAZ and HAZ local dissolution of strengthening particles into the aluminum matrix and a reduction in the dislocation density caused decreasing the hardness in this regions. The difference between hardness for the corresponding points at each side (advance and retreat sides) can be interpreted as the same direction of rotation velocity vector and the forward motion in the advance side AS gave a higher heating than on retreat side RS. The value of hardness for BM is 170 HV, in this work it is noted that when increasing the SWI depth the hardness was increased whereas the highest hardness in center of NZ reached to 164.8 HV when SWI depth is 0.25 mm in the specimen no. 17 and the lowest value is 155.3 HV at SWI depth 0.15 mm. That is means when an increase in SWI depth, the heat input increases and dynamic plastic deformation increases. Specimen no.15 has a lack of penetration defect but do not affect the value of hardness which were close to other samples and also have the same behavior of all samples in general i.e W shape.

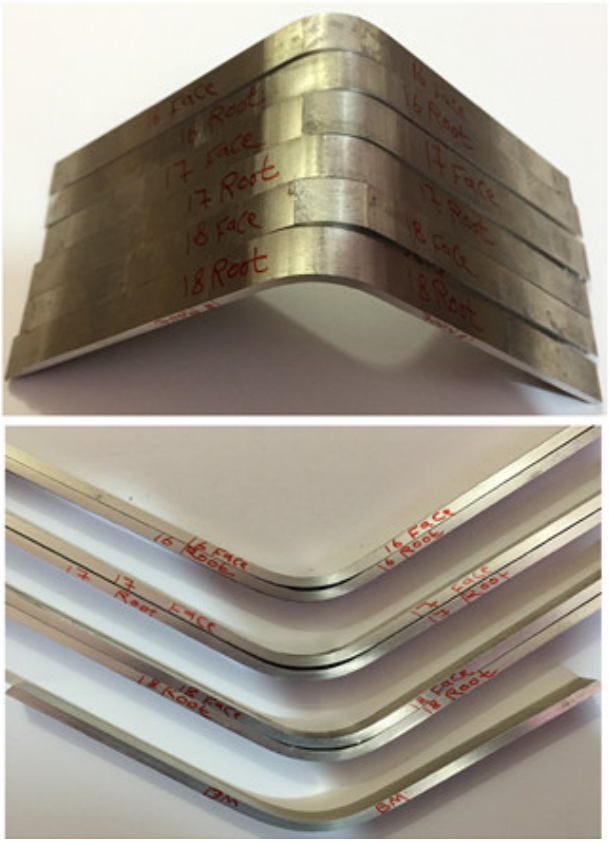

Figure 16: Specimens after bending test

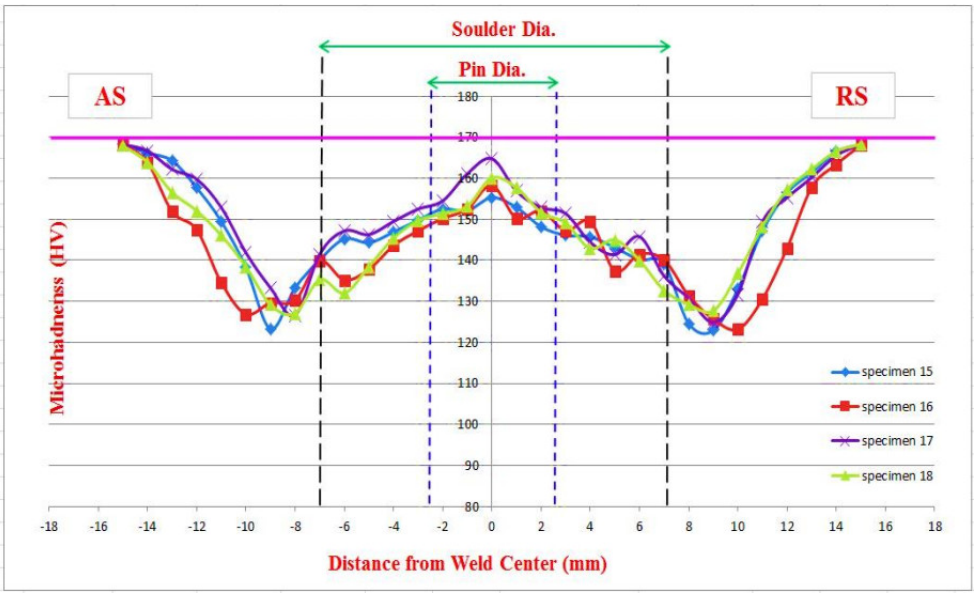

Figure 17: Micro-hardness distribution through cross section of FSW welds at different SWI depth

7. Conclusions

According to the previous discussion of the obtained result the following conclusion can be extracted:

1. Visible and invisible defect are observed when SWI depth in range of (0.05-0.15) mm.
2. The defect-free joints were achieved when SWI depth was in the range (0.2-0.3) mm.

3. Fully re-crystallized in the weld center and equiaxed grain in smaller size, and in the TMAZ there is no dynamic recrystallization, and instead, the grains were elongated and typically of a different orientation than those in the base metal, while there is no significant change in grain size or orientation in the HAZ when compared to BM .
4. The maximum value of tensile strength was 484.8 MPa when the SWI depth was 0.25 mm.
5. Micro-hardness in the welding zones is less than in the BM, while the micro-hardness in SZ is higher than in TMAZ and HAZ. Increasing the SWI depth leads to increase the hardness in NZ and the maximum value of HV was 164.8 in specimen no. 17.
6. The maximum value of bending stress and bending angle was 835 MPa and 107° respectively when the SWI depth was 0.25 mm, a slight difference between the face and root bending is resulted.
7. SWI depth was important parameters in friction stir welding process through its impact on the mechanical properties for weld joint, so the best value of SWI depth was 0.25 mm.

Acknowledgements

We thank everyone who helped me to carry out this research from people and institutions.

References

[1] Cam, G. (2011) 'Friction stir welded structural materials eyond Al-alloys', International Materials Reviews, 56(1), pp. 1–48.

[2] Derazkola, H. A., Elyasi, M. and Hossienzadeh, M. (2016) 'Effects of friction stir welding tool plunge depth on microstructure and texture evolution of AA1100 to A441 AISI joint', Int J Advanced Design and Manufacturing Technology, 9 (1), p. 13.

[3] Đurđanović, M. B. et al. (2009) 'Heat Generation during Friction Stir Welding Process', Tribology in industry, 31(1), pp. 8–14.

[4] Elangovan, K., Balasubramanian, V. and Babu, S. (2008) 'Developing An Empirical Relationship to Predict Tensile Strength of Friction Stir Welded AA2219 Aluminum Alloy', Journal of Materials Engineering and Performance, 17(6), pp. 820–830.

[5] Groover, M. P. (2010) 'Fundamentals of Modern Manufacturing Materials, Processes, and Systems'. Fourth ed, edited by M. McDonald and L. Sapira. United States: JOHN WILEY & SONS, INC, P. 737.

[6] Imam M., Sun Y., Fujii H., Ma N., Tsutsumi S., and Murakawa H. (2016) 'Microstructural Characteristics and Mechanical Properties of Friction Stir Welded Thick 5083 Aluminum Alloy', Metallurgical and Materials Transactions A: Physical Metallurgy and Materials Science. Springer US.

[7] Khansha, Z.-A., Saeri, M. and Otroj, S. (2015) 'Study of Stress Corrosion Cracking of Aa7075-T6 Aluminum Alloy By Chromate Coatings', Indian Journal of Fundamental and applied life sciences, 5, pp. 4129–4139.

[8] Kumar, H. M. A. and Ramana, V. V. (2014) 'An Overview of Friction Stir Welding (FSW): A New Perspective', International Journal of Engineering and Science, 4(6), pp. 1–4.

[9] Lohwasser, D. and Chen, Z. (2010) 'Friction Stir Welding From Basics to Applications'. Woodhead Publishing Limited, Abington Hall, Granta Park, Great Abington, Cambridge CB21 6AH, UK.

[10] Mishra, R. S. and Mahoney, M. W. (2007) 'Friction Stir Welding and Processing', ASM International, pp. 368.

[11] Polmear, I. J. (2004) 'Aluminium Alloys-A Century of Age Hardening', Materials forum, 28, pp. 1–14.

[12] Ramulu, P. J., Narayanan, R. G. and Kailas, S. V. (2013) 'Forming limit investigation of friction stir welded sheets: Influence of shoulder diameter and plunge depth', International Journal of Advanced Manufacturing Technology, 69(9–12), pp. 2757–2772.

[13] Rengarajan, S. and Rao, V. S. (2015) 'Characteristics of AA7075-T6 and AA6061-T6 Friction Welded Joints', Transactions of the Canadian Society for Mechanical Engineering, 39(4), pp. 845–854.

[14] Schwartz, M. (2011) Innovations in Materials Manufacturing, Fabrication, and Environmental Safety. Printed in the United States of America on acid-free paper: 2011 by Taylor and Francis Group, LLC.

[15] Shi, L. and Wu, C. S. (2017) 'Transient model of heat transfer and material flow at different stages of friction stir welding process', Journal of Manufacturing Processes, 25, pp. 323–339.

[16] Thomas, W. M., Johnson, K. I. and Wiesner, C. S. (2003) 'Friction stir welding-recent developments in tool and process technologies', Advanced Engineering Materials, 5(7), pp. 485–490.

[17] Zhang, H. J. et al. (2016) 'Improving the structure-property of aluminum alloy friction stir weld by using a non-shoulder-plunge welding tool', International Journal of Advanced Manufacturing Technology, 87(1–4), pp. 1095–1104.

[18] Zevanathan, C. and Babu. (2013) 'Effect of Plunge Depth on Friction Stir Welding of Al 6063', in 2nd International Conference on Advanced Manufacturing and Automation (INCAMA-2013), pp. 482–485.

Abbreviations

AA	American Association
Al	Aluminium
AS	Advance side
ASTM	American Society for Testing and Materials
BM	Base metal
CCW	Counter clock wise
CTFE	Cylindrical Thread Flat End
CW	Clock wise

EDM	Electrical Discharge Machine
FSW	Friction stir welding
HAZ	Heat affected zone
HV	Hardness Vickers
KB	Kissing Bond
LHT	Left Hand Thread
NZ	Nugget zone
RPM	Revolution Per Minute
RS	Retreat Side
SPD	Shoulder Plunge Depth
SWI	Shoulder-Workpiece Interference
SZ	Stir Zone
TMAZ	Thermal Mechanical Affected Zone
TRS	Tool rotational speed
TWI	The Welding Institute
UTS	Ultimate Tensile Strength
WP	Work piece
WPs	Work pieces
WS	Welding speed
WZ	Welding zone

تأثير عمق التداخل ما بين الكتف وقطعة العمل على جودة اللحام بالاحتكاك والخلط لسبائك الألمنيوم **AA7075-T6**

***عباس اكرم عباس*[1،*]، *حازم حاتم عبد الكاظم*[2]**

[1] *قسم هندسة الميكانيك، جامعة بغداد، بغداد، العراق، abbas.akram.aa@gmail.com*

[2] *وزارة التربية، المديرية العامة للتعليم المهني، بغداد، العراق، hhabdulkadhum@gmail.com*

[*] *الباحث الممثل: عباس اكرم عباس، abbas.akram.aa@gmail.com*

نشر في: 31 آذار 2019

الخلاصة – تم تطبيق عملية لحام الاحتكاك والخلط على صفائح من سبيكة الألمنيوم العالية المتانة AA7075-T6 ذات سمك 3 ملمتر تم دراسة تأثير عمق التداخل ما بين كتف العدة وسطح قطعة العمل على جودة اللحام ومدى تأثيرها على الخواص الميكانيكية والبنية المجهرية للمفاصل الملحومة باستخدام عدة لحام مركّبة تتكون من كتف مقعّر مصنوع من فولاذ العدة (H13) و ننوء اسطواني مسنن وبخطوة تسنين (1) ملم صنع من سبيكة نيكل-كوبلت (MP159). أبعاد عدة اللحام هي 14 ملم لقطر الكتف و 5 ملم لقطر النتوء و2.7 ملم لطول النتوء. تم اختيار سرعة دوران العدة 981 دورة في الدقيقة وسرعة اللحام 169 ملم/ دقيقة، و زاوية ميل قطعة العمل 2°. تم اختيار مدى من عمق التداخل ما بين كتف عدة اللحام و قطعة العمل (0.05، 0.1، 0.15، 0.2، 0.25، 0.3) ملم. تم اختبار الملحومات بواسطة الفحص البصري وفحص الأشعة السينية، وأيضا التقييم الماكروي والمايكروي لخصائص البنية المجهرية لمناطق اللحام. وأجريت بعض الفحوصات لتقييم الخواص الميكانيكية للمفاصل الملحومة ومن ضمنها فحص الشد والحني وقياس الصلادة الدقيقة. أظهرت النتائج عند عمق التداخل 0.05 ملم ظهور عيب نقص في امتلاء خط اللحام عند سطح اللحام، وظهور عيب النفق غير مرئي وعيب نقص الاختراق في جذر منطقة الخلط عند عمق التداخل 0.1 ملم و 0.15 ملم. في حين تم الحصول على الملحومات الخالية من العيوب عند عمق التداخل (0.2 ، 0.25 ، 0.3) ملم. تم الحصول على كفاءة لحام للملحومات الخالية من العيوب في المدى (85.3-92.3٪) اعتمادًا على اقصى مقاومة شد بالمقارنة مع اقصى مقاومة شد للمعدن الأصلي.

الكلمات الرئيسية – AA7075، لحام الاحتكاك والخلط، عمق التداخل ما بين الكتف وقطعة العمل، عمق الغطس، المثبت.